Elaboration of Metallic oxide nanopowder Fe doped ZnO

Amel Boulassel / Physics Laboratory of Condensed Matter and nanomaterials (PLCMN), Jijel University BP 98, Ouled aissa, Jijel 18000, Algéria.
e-mail address :amelboulassel@yahoo.fr

Zahi Takkouk / *materials study laboratory (MSL), Jijel University BP 98, Ouled aissa, Jijel 18000, Algéria*

***Abstract* — Among the methods of elaboration the metallic oxide nanopowders based on green chemistry,co-precipitation is a simple process used for industrial production in different sectors .It is the preparation of an aqueous solution containing the desired cation then mixing with a solution containing the precipitating agent .the precipitate is then separated from the liquid by filtration, washing, drying and then thermally decomposing to yield the desired product.**

Our study focused on pure and Fe doped ZnO nanopowders ($Zn_{1-x}Fe_xO$, x=0.0,0.005,0.02,0.05 and 0.15) prepared by co-precipitation methode at room temperature with zinc acetate as a zinc source. Samples were analyzed by X-ray diffraction (XRD), scanning electron microscope (SEM), infrared spectroscopy IR and UV-visible spectroscopy.

All powders are polycrystalline with a hexagonal (wurtzite), grain powders were nanometric sizes. From a doping level the secondary phase ZnFe2O4 appear and found a decrease in grain size and increase internal stresses with increasing the concentration of Fe dopant. SEM images show the existence of settlements powder particles in spherical form. IR infrared spectroscopy we identified in the specific vibration and the peak characteristic of the ZnO matrix, Zn-O binding was clearly observed at around 470 cm^{-1}.the Study of the optical properties of the samples clearly shows the doping effect on the optical absorption spectra and allowed us to determine the optical absorption edge and the width of the gap.

Keywords— ***ZnO, $ZnFe_2O_4$, co-précipitation, the structural properties, nanopowder.***

I. INTRODUCTION

Compared to materials called conventional, nanomaterials exhibit new physical properties which open promising perspectives in terms of application, whether in the field of magnetism, mechanics, catalysis and optics.

ZnO is one of the most important nanomaterials for industrial and biotechnological applications. As it has wide bandgap (3.27 eV) at room temperature and large exciton binding energy (60 meV) which is much higher than that of some commonly used materials such as ZnSe (20 meV) and GaN (25 meV). ZnO is used usually doped with different types of ions, such as Sn, Ga, In, Sn, Al,Fe and Ni to improve its properties TCO (transparent conductive oxide).

Non-toxicity and abundance of ZnO on earth makes him an ideal candidate used in the field of optoelectronics and photovoltaics. It can be used in several applications in various scientific and industrial fields such as piezoelectric transducers, waveguides, gas detectors [1], conductive transparent electrodes, varistors [2]. It is important to note that the zinc oxide in its pigmentary form, it diffuses and strongly absorbs ultraviolet radiation [3].

Among many of the development of micro or nanostructures powdered materials techniques, methods exist for cheaper and more accessible development include the sol-gel synthesis and Co-precipitation which has been chosen for our study because it is less expensive, simple to implement. As part of this work, we focused on the study of the influence of the concentration of Fe on the structural and optical properties of ZnO nanopowders obtained through co-precipitation.

II. EXPERIMENTAL PROCEDURE

II.1.Samples preparation

The ZnO nanopowder was prepared by co-precipitation method. Zinc acetate -dehydrate [$Zn(CH_3COO)_2$. $2H_2O$], Iron chloride dihydrate[$FeCl_2.2H_2O$], Oxalic acid dehydrate [$C_2H_2O_2.2H_2O$] purchased from Sigma Aldrich company were used as precursor, Fe doping source, precipitating agent respectively without further purification. Distilled water and Acetic acid was used for aqueous solution preparation (as solvent and agent).Pure and doped ZnO nanopowder was synthesized as follows: the appropriate proportion of $Zn(CH_3COO)_2.2H_2O$, $FeCl_2.2H_2O$, and $C_2H_2O_2.2H_2O$ were completely dissolved in a solution of 90 ml distilled water and 3 ml acetic acid. Mole ratios of Fe^{2+} to Zn^{2+}were 0.0%, 0.5%, 2%, 5% and 15%. The aqueous solution was then stirred vigorously for about 4h at roome temperature in order to mix the solution uniformly.The obtained mixture was kept for about 17h without magnetic stirring. The precipitate was filtered, washed with distilled water for several times in order to remove Cl^- ions (this step is misplaced for pure ZnO preparation) and then dried in about 80°C at atmospheric pressure for 2h. The as -synthesized pure and doped nanocrystalline ZnO powder was further calcined in air at 800°C for 1h.

After the elaboration of the ZnO nanopowders, he then proceeded to their characterization by X-ray diffraction (XRD-X 'Pert Pro), scanning electron microscope (FEI QUANTA 200 type), Infrared spectroscopy (400 cm- 1-4000 cm-1) and type spectrophotometer UV-Vis SCHIMADZU 1601.

III.Results and discussion

III.1.Analysis by X-ray diffraction:

Figure 1 shows the XRD patterns of pure and Fe doped ZnO nanopowders ($Zn_{1-x}Fe_xO$, x=0.0,0.005,0.02,0.05 and 0.15) prepared by co-precipitation methode and calcined at 800 ° C for 1 hour. It is observed that all powders are polycrystalline of hexagonal Wurtzite structure (space group P63mc) that is known ZnO structure., from doping level of 5% Fe in addition to the peaks characteristics of the hexagonal phase of ZnO, is observed additional peaks occur at diffraction angles 2θ(°) = 29.93 °, 35.35 °, 42.61 °, 53.16 °, 62.15 °. These peaks are very similar to the diffraction peaks of the $ZnFe_2O_4$ phase comparing with the JSPDS card 1997. The planes responsible for observed diffractions are (220), (311), (400), (511) and (440) respectively. It is noted a decrease in ZnO peak intensities during the occurrence of the secondary phase, which is corresponds to the degradation of the crystal quality of the ZnO matrix.

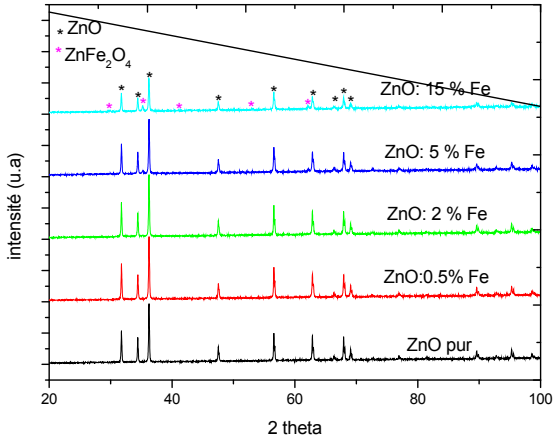

Fig.1.XRD patterns of pure ZnO powder and Fe-doped ZnO powder samples at different % Fe

There is also a shift of ZnFe2O4 (311) peaks at small angles of diffraction 2θ (Fig. 2). Similar results were found by R.ELILARASSI et al), it is explained by the incorporation of dopants ions in host materials network [6].

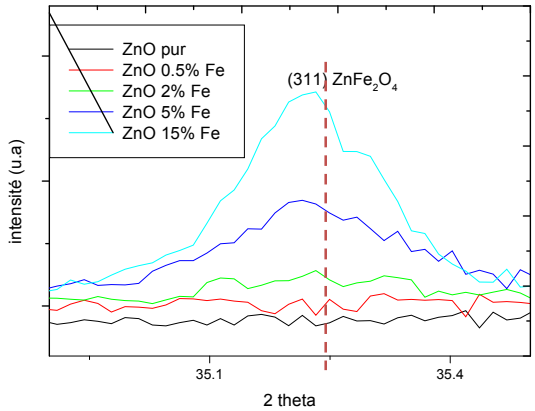

Fig.2.Intensity and peak shift $ZnFe_2O_4$ (311) as a function of doping level.

The average grain size was determined using the formula of Scherrer for the strongest peak (101).

$$D = \frac{k.\lambda}{\beta.\cos\theta} \qquad (1)$$

Where D is the crystalline size,λ is the wavelength of the incident X-ray (1.54 A°), θ is the bragg's and β is the full width at half maximum (FWHM).

The relationship linking the interplanar distances of the planets (hkl) with crystallographic parameters **a** and **c** is:

$$\frac{1}{d_{hkl}^2} = \frac{4}{3}\left(\frac{h^2 + hk + k^2}{a^2}\right) + \frac{l^2}{c^2} \qquad (2)$$

In this formula, we can determine the parameter **c** by taking the plans for which h = k = 0, l = 2. The last formula becomes

$$d_{002} = \frac{c}{2}, \qquad c = \frac{\lambda}{\sin\theta_{002}}$$

and also the parameter **a** for the plans **h = 1, k = l = 0**.

$$d_{100} = \frac{\sqrt{3}}{2}a, \quad a = \frac{\lambda}{\sqrt{3}\sin\theta_{100}}$$

The evolution of grain size and lattice parameters **a** and **c** as a function of doping Fe is illustrated in Figures 3 and 4 respectively.

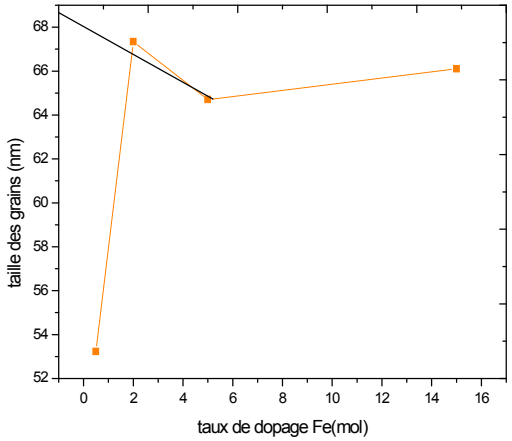

Fig.3. Evolution of particle size depending on the doping level in Fe.

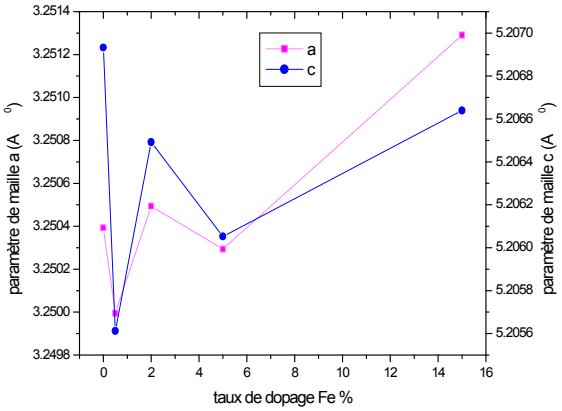

Fig.4. Evolution of the lattice parameters a function of doping.

At low concentration of dopant the grain size increases with the doping level, this result confirms the incorporation of dopant in the ZnO matrix substitutional positions.

The addition of dopant proportion causes a decrease in grain size. This reduction caused by the emergence of other plans, or by the formation of the secondary phase which hinders grain growth. The reduction of the grain size with the doping level of Fe is found by other researchers [7.8].

ZnO doped Fe lattice parameters increases with the doping level, so the substitution of Fe caused an expansion of the crystal lattice [9] knowing r_{Zn2+} = 0.074 nm <rFe2 + = 0.077 nm [10].

The constraints were estimated from the XRD diffraction patterns, exploiting the offset of the strongest peak position (101) against the diffraction angle on this peak for pure ZnO by the following expressions [5]:

$$\varepsilon_s = -\Delta\theta_{(101)} \cot g\theta_{(101)} \qquad (3)$$

$$\sigma_{st} = 3\varepsilon_s B \qquad (4)$$

Such as:

$\boldsymbol{\varepsilon_s}$: microstrain at the mesh.

$\boldsymbol{\sigma_{st}}$: stress (GPa).

B: average compressibility ZnO module (B=143GPa[11]).

$\boldsymbol{\theta}$: Bragg angle of diffraction (rad).

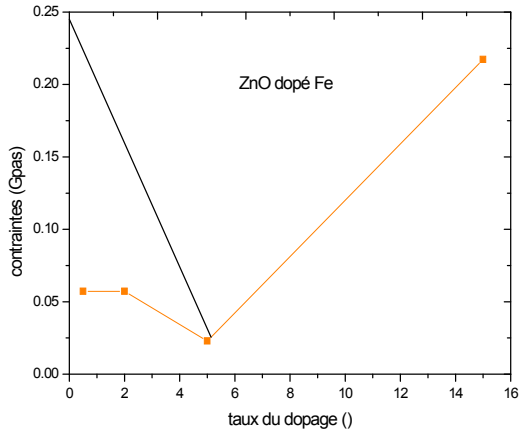

Fig.5. constraints values as a function of Fe doping concentration.

At low level doping stresses increase with the doping level Knowing $r_{Zn}^{2+} > r_{Fe}^{2+}$; this evolution is due to the occupation of constitutional site by Fe ions. While increasing constraints from a certain percentage is interpreted by the saturation of substitutional site forcing iron ions occupy interstitial sites.

III.2.Analysis by Scanning Electron Microscopy:

The scanning electron microscope gives us information of the doping effect on the overall morphology. SEM images of the powders ($Zn_{1-x}Fe_xO$; x = 0; 0.15) are shown in FIG if below:

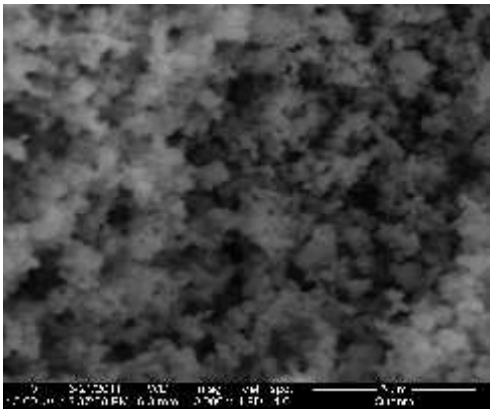

(a)

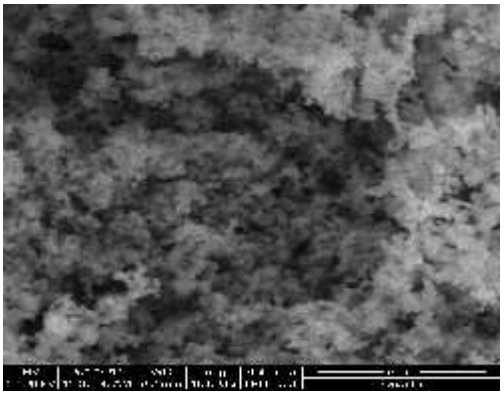

(b)

Fig.6.SEM images of ZnO: (a) undoped, (b) doped 15% Fe.

It is observed that the particle shape is spherical with a homogeneous distribution.

III.3.Analysis by Infrared Spectroscopy

IR spectra (Fig. 7) of all the powders clearly show the existence of a vibration mode located at 450-550 cm^{-1}. .this mode is related to the vibration of elongation of the Zn-O bond. The appearance of this absorption band confirms the formation of the wurtzite phase of ZnO[12-13]. A large localized absorption band around 3500 cm -1 is assigned to O-

H bonds, which may be due to moisture. We also note a band absorption around 2350 cm^{-1} corresponding to the presence of carbon dioxide (CO_2) in our sample (absorption from the atmosphere).

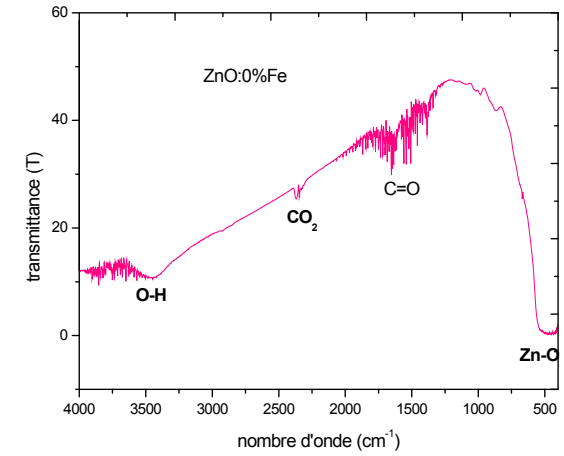

(a)

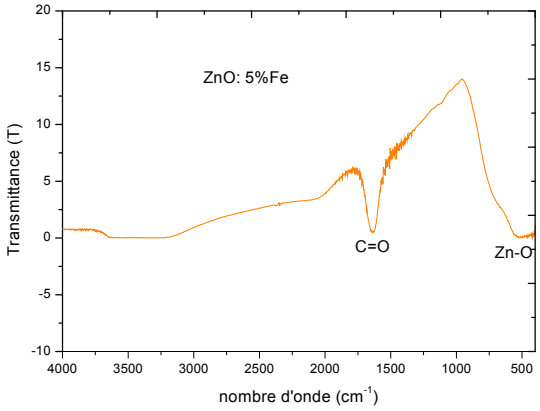

(b)

Fig. 7: FTIR spectra of ZnO nanopowder: (a)undoped, (b) doped 5% Fe.

III.4.Optical characterizations (UV-Vis)

The fundamental absorption corresponds to the excitation of an electron from the band Valencia to the conduction band and this brutal threshold of absorption can be used to determine the value of the band gap (gap).

$$Eg(eV) = 1240/\lambda(nm).$$

The optical absorption spectra of ZnO doped Fe and calcined at 800 ° C and the variation of the optical gap as a function of doping level is shown below:

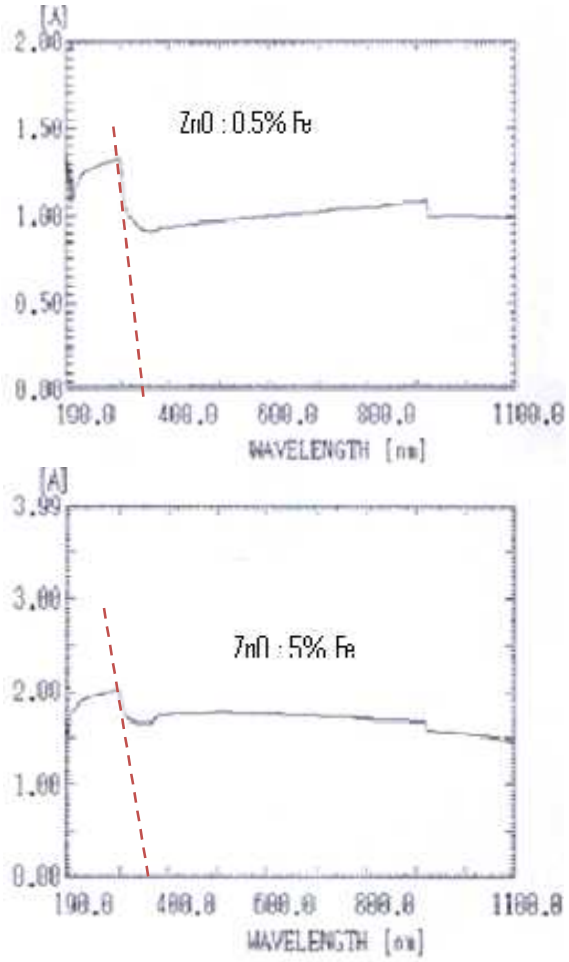

Fig. 8: absorption spectra of ZnO doped iron.

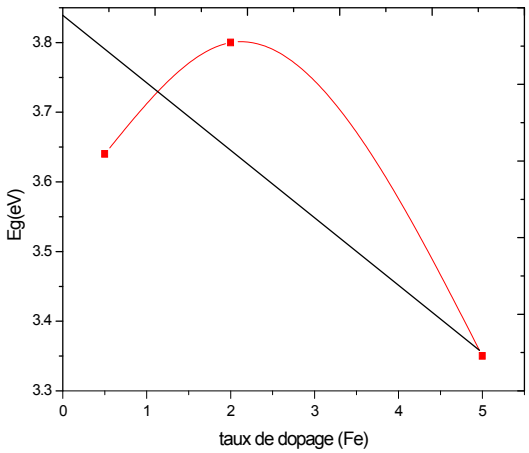

Fig. 9. Gap of ZnO Dependence with doping level Fe.

As can be seen, the gap nanopowders decrease with increasing doping. This decrease is mainly due to distortions caused in the network following the introduction of impurities (doping) and the increase of the concentration of free electrons. This is possibly the result of occupying interstitial sites by the dopant atoms because they represent the major native donor in ZnO nanopowders [14].

Conclusion

We succeeded to elaborate ZnO nanopowders pure and doped Fe by the co-precipitation method. Structural analysis using the DRX technique, we demonstrated Fe dopant solubility in the ZnO matrix and also the presence of the secondary phase from a doping level. SEM images showing the existence of settlements grain in spherical shapes. From IR infrared spectroscopy we found characteristic peaks of the semiconductor ZnO (Zn-O bond). From IR infrared spectroscopy we found characteristic peaks of the semiconductor ZnO (Zn-O bond).

References

[1] Z. Ling, C. Leoch, R. Freer, "Heterojunction gas sensors for environmental NO_2 and CO_2 monitoring", J. Eur. Ceram. Soc. 21 (2001) 1977–1980.

[2] L. Gao, Q. Li, W. Luan, H. Kawaoka, T. Sekino, K. Niihara, J. Am. Ceram. Soc. 85 (4) (2002) 1016.

[3] A. Djelloul and R.A. Rabadanov, 'Thermochemical and Green Luminescence Analysis of Zinc Oxide Thin Films Grown on Sapphire by Chemical Vapor Deposition', Turkish Journal of Physics, Vol. 28, N°5, pp.309 – 323, 2004.

[4] J.E. Rodriguez, A.C. Caballero, Controlled precipitation methods: formation mechanism of ZnO nanoparticles, J. Eur. Ceram. Soc. 21 (2001)925–930.

[5] M.El-Hilo, A.A.Dakhel , A.Y.Ali-Mohamed /Journal of Magnetism and Magnetic Materials 321 (2009) 2279–2283.

[6] J.Cui,Q.Zeng.U.J.Gibson,J.Appl.phys.99(2006)08 M 113.

[7] J.Hays,et al,J.phys.condens Matter 19(2007)266203.

[8] J.Hays,A.punnoose,R.Balder,M.H.Englehard,J.Peloquin.K.M.REDDY. phys.rev.B72(200 5)075203.

[9] C.B.Fitzgeerald,M.VenKatesan,A.P.Douvalis,J.Appl.Phys.95(2004)739 0.

[10] Rosari Saleh, Suhendro Purbo Prakoso, Adel Fishli, The influence of Fe doping on the structural, magnetic and optical properties of nanocrystalline ZnO particles, Journal of Magnetism and Magnetic Materials 324 (2012) 665–670

[11] B. Zhang, X.T. Zhang, H.C. Gong, Physics Letters A, 2008, 372: 2300–2303

[12] Liu-Niu Tonga, Xian-Mei Heb, Huai-Bin Hana, Jin-Lian Hua, Ai-Lin Xia a, Yan Tongc / Solid State Communications 150 (2010) 1112-1116.

[13] C.F.Cline,D.R.Stephens,J.Appl.Phys.36(1965)2869.

[14] N. Smirnova, A. Eremenko, O. Rusina, W. Hopp, L. Spanhel, ''Synthesis and Characterization of Photocatalytic Porous Fe^{3+}/TiO_2 Layers on Glass '', J. Sol–Gel Sci. Technol. 21 (2001) 109-113.